Towards waste refinery: Co-feeding HDPE pyrolysis waxes with VGO into the catalytic cracking unit

Elena Rodríguez, Roberto Palos, Alazne Gutiérrez*, David Trueba, José M. Arandes, Javier Bilbao

Department of Chemical Engineering, University of the Basque Country UPV/EHU, PO Box 644, 48080 Bilbao, Spain

(*) corresponding author: alazne.gutierrez@ehu.eus

ABSTRACT

The co-feeding of high-density polyethylene pyrolysis waxes (HDPE waxes) with vacuum gasoil (VGO) on the catalytic cracking has been investigated. Runs have been conducted by feeding a blend of HDPE waxes/VGO (1/4 in mass) to a laboratory-scale reactor that mimics the behavior of the riser reactor of the industrial FCC unit. Tested operating conditions have been the following: 500-560 ºC; catalyst to oil mass ratio (C/O), 3-7 g_{cat} g_{feed}^{-1}; and, contact time, 6 s. The comparison of obtained results, i.e., yield and composition of the fractions, in the cracking of the blend with those obtained in the cracking of the VGO and HDPE waxes separately, has exposed the existence of synergetic mechanisms. This way, the cracking of the blend produces a more olefinic gaseous fraction and a naphtha with higher content of *iso*-paraffins and olefins and lower of aromatics, together with a comparable yield of coke.

Keywords: Cracking; FCC unit; Waste plastic; Non-conventional fuels; Waste refinery

1. Introduction

Global production of plastic has steadily increased in the last 50 years reaching a production of more than 359 million of tones in 2018 [1]. Today, the average rate of waste plastic generation per person living in developed countries is estimated at 7 kg each year, mostly in the form of packaging; whereas in the most polluting countries it increases up to 72 kg per person [2]. However, current recovery and recycling routes remain insufficient and millions of tons of plastics end up in landfills and oceans entailing risks to ecosystems, biodiversity and food availability [3].

Consequently, new routes must be implemented in order to achieve higher recycling degrees, being the thermochemical routes, i.e., gasification and pyrolysis, those that attract greater attention for the large-scale plastics valorization [4,5]. The interest of gasification lies in the feasibility of producing energy carriers (hydrogen), as well as fuels and chemicals (methanol, dimethyl ether, among others) in a subsequent catalytic stage from the syngas [6,7]. However, pyrolysis shows a higher efficiency in the goal of eliminating plastic waste, with higher production rates that entail a higher overall carbon efficiency, while generally being simpler to build and operate [5,8–10].

The pyrolysis of polyolefins has been extensively studied in the literature, as they cover 2/3 of the waste plastics found in the municipal solid waste. Its versatility allows for establishing the optimal conditions for the recovery of monomers and chemicals (specifically aromatics) in the valorization of polyolefins [11]. Moreover, the production of liquid oil or waxes has a great potential since their calorific value is comparable with that of commercial fuels [8,12]. Fivga and Dimitriou [13] have determined that with the appropriate scale of production, the fuel production costs using plastics pyrolysis-derived oils is lower than the existing market prices of residual fuel oil.

Furthermore, polyolefins can be co-fed with different types of biomass, boosting the synergies in the cracking mechanisms resulting in higher quality oils when comparing with those obtained with the feeds separately [14,15]. Several authors have studied the performance of diesel engines fueled with neat plastic oil [16,17] and blended with conventional diesel [18,19]. There have been also used different types of catalysts, e.g., clay-based [20–22], or zeolite-based catalysts [23–25], both in-situ or ex-situ in the pyrolysis stage to improve the composition of obtained oil or to adjust it to the requirements of the market of automotive fuels [26–28].

In spite of the technological advances, the commercialization of a recycling technology to convert plastics into fuels that lays on the pyrolysis of waste plastics has not reached significant levels of profitability yet. Its main drawbacks are: (i) the lack of facilities for the production of high-quality fuels; and (ii) the difficulties for launching in the market these unconventional fuels, as fuels market is well established and quite delimited. In this scenario, a reasonable strategy would be to consider the capacity of the oil refining industry to adequate the composition of the waste plastic pyrolysis oil. Therefore, the upgrading of waste plastics by means of a two-stage process appears as an attractive option: a first stage of thermal pyrolysis, which could be done in a delocalized way in small units located nearby the waste plastics collection points, in order to obtain an appropriate stream to be submitted to a second upgrading stage in refinery (Waste-refinery). In this latter stage, the reaction and separation units already depreciated and commonly available in refineries for the production of fuels will be used, to adapt the composition of obtained products to the legal requirements.

The pyrolysis of the different polyolefins (high and low-density polyethylene, polypropylene, etc.) does not show notorious differences. Nonetheless, the yields and composition of the product fractions obtained in the pyrolysis of polyolefins do strongly

depend on the type of reactor used (batch, fixed, bed, fluidized bed, spouted bed, microwave, etc.) and on the chosen operating conditions (continuous or discontinuous regime, temperature, heating rate, residence time of the volatiles, amount and properties of the catalyst, etc.) [4,8,9,29,30]. This way, operating at fast pyrolysis conditions the yield of oil is maximized, while an excessive production of char is avoided. The conical spouted bed reactor (CSBR) shows appropriate characteristics for the fast pyrolysis of waste plastics given the short residence time of the volatiles (ca. 1 cs) and the cyclic and vigorous movement of the particles. These conditions guarantee the isothermicity of the bed, ease the volatilization of the molten plastic and avoid the defluidization phenomena and the formation of char [31]. Using the CSBR a maximum yield of waxes (C_{21+}) of 90 wt% is obtained at 450 ºC in the pyrolysis of HDPE when operating in discontinuous regime for the solid [32]. Elordi et al. [33] consider that the temperature of 500 ºC allows for a continuous feeding of HDPE and stable behavior of the system. Under these conditions, the yield of waxes is of 68 wt%, and those of gasoil (C_{12}-C_{20}), naphtha (C_5-C_{11}) and gas (C_1-C_4) fractions are of 25, 5 and 2 wt%, respectively. Besides, the properties and composition of these waxes are the optimal ones to be co-fed to a refinery FCC unit [34]. FCC unit has a great capacity (a standard unit can easily manage 50000 barrels day^{-1}) and versatility for the co-feeding of secondary refinery streams [35,36]. The catalytic cracking of raw HDPE waxes has been studied by Rodríguez et al. [37,38] under conditions similar to those of the industrial FCC riser reactor, obtaining high yields of liquefied petroleum gases (LPG) and naphtha fractions. Furthermore, a more olefinic and less aromatic naphtha fraction has been obtained when comparing it with that obtained in the cracking of the vacuum gasoil (VGO, current feed of the FCC unit).

Based on all the previous, the oil refining industry could be a cornerstone for the upgrading of waste plastics. Hence, we have investigated the catalytic cracking of HDPE

96 waxes by co-feeding them with the conventional FCC unit feed (VGO). This work tackles
97 a more realistic approach given the big capacity of FCC units, considering that with the
98 co-feeding of 20 wt% of HDPE waxes the valorization of the polyolefins discarded in a
99 large geographical area would be covered. With the purpose of obtaining results attractive
100 for the industry, experimental tests have been carried out in a unit that mimics the behavior
101 of the industrial FCC unit; even using a commercial equilibrated catalyst in the runs.
102 Moreover, the yields and composition of the product streams have been analyzed in-detail
103 to properly assess their incorporation to refinery pools. The studio allows for determining
104 the synergy among the cracking mechanisms of both streams and for comparing the yields
105 and composition of the fractions of products (specifically of the naphtha fraction) with
106 the results obtained in the cracking of the VGO.

107 **2. Experimental**

108 *2.1. Materials*

109 High-density polyethylene (HDPE) waxes have been obtained by fast pyrolysis of raw
110 HDPE, which has been supplied by Dow Chemical (Tarragona, Spain), at 500 ºC in a
111 continuous pyrolysis plant equipped with a conical spouted bed reactor [33]. At these
112 conditions, at which the energy requirement of the pyrolysis is reduced, the yield of waxes
113 is of 68 wt%. Moreover, the other product fractions have an interesting composition for
114 their incorporation in the refinery streams of medium distillates, naphtha and light olefins,
115 given their olefinic nature [33]. The composition of the HDPE waxes has been determined
116 by means of gas chromatography following the procedure described in a previous work
117 [37], obtaining that they are composed of mono- and di-unsaturated olefins (48.20 and
118 19.37 wt%, respectively) and paraffins (32.43 wt%). Table S1 in the Supplementary
119 Material shows the composition and main properties of the HDPE waxes.

120 Vacuum gasoil (VGO) has been directly supplied by Petronor Refinery (Muskiz, Spain)
121 and consists on a broad vacuum distillate with a boiling range of 190–598 ºC, and which
122 is a base feed for the fluid catalytic cracking (FCC) unit of the refinery. As in the case of
123 the HDPE waxes, the composition of the VGO has been already determined in a previous
124 work [37], being aromatics the main compounds (62.3 wt%) followed by naphthenes
125 (29.2 wt%) and paraffins (8.5 wt%). The composition and main physicochemical
126 properties of the VGO have been collected in Table S2 in the Supplementary Material.

127 The catalyst used is a commercial equilibrium FCC catalyst, which has being used in the
128 FCC unit at the Petronor Refinery. It is a catalyst incorporating a 13.8 wt% of a stabilized
129 form of USY zeolite embedded in a meso- and macroporous matrix made of various
130 alumina and silica sources. Main properties of the catalyst are tabulated in Table S3 in the
131 Supplementary Material, whereas an in-deep characterization of the catalyst can be found
132 elsewhere [39]. It should be highlighted that the hierarchical porous structure of the
133 catalyst is appropriate to promote the diffusion and cracking of the linear long chains of
134 the waxes.

135 *2.2. Reaction equipment*

136 The runs have been performed in a laboratory-scale CREC riser simulator reactor [40],
137 which has been designed to reproduce the behavior of the industrial FCC unit. The reactor
138 is equipped with an impeller located in the upper side of the reactor that rotates at 5700
139 rpm producing the fluidization of the catalyst particles within the basket and the
140 recirculation of the hydrocarbon species. Additional information about the reactor and the
141 general operating procedure can be found in the literature [41,42]. In short, a run consists
142 on the injection of the feed by means of a syringe, which vaporizes at the entrance of the
143 reactor and circulates through the catalytic bed (at a preset temperature and catalyst/oil

144 ratio) during the short and preset reaction time. Once the reaction time is elapsed, the
145 reaction medium is sucked into the chromatographic analysis system.

146 The experimental tests have been carried out under the following conditions, which have
147 been selected according to the reality of the industrial FCC unit: 500–560 ºC; catalyst/oil
148 (C/O) mass ratio, 3-7 $g_{cat}\ g_{feed}^{-1}$; and, contact time, 6 s. To ensure both the reproducibility
149 and the reliability of the obtained data, each run has been repeated at least three times. It
150 should be underlined that experimental error amounted maximum 2 %.

151 *2.3. Product analysis*

152 Obtained products have been analyzed by means of gas chromatography in an Agilent
153 Technologies 7890A GC system equipped with an FID detector and a HP-PONA capillary
154 column (100 % dimethylpolysiloxane, 50 m × 0.2 mm × 0.5 μm). The GC oven
155 temperature has been programmed as follows: -30 °C (hold for 3 min), raised to 235 °C
156 at a heating rate of 15 °C min^{-1} (hold for 1 min) and raised up to 320 ºC following a ramp
157 of 30 ºC min^{-1}. The sample injector and detector have been maintained at 250 and 340 °C,
158 respectively. Additionally, the products have been lumped according to a boiling point
159 criteria basis: dry gas (C_1–C_2), liquefied petroleum gas (LPG, C_3–C_4), naphtha (C_5–C_{12}),
160 light cycle oil (LCO, C_{13}–C_{20}), and heavy cycle oil (HCO, C_{20+}). On the other hand, the
161 amount of coke deposited on the catalyst has been measured by means of temperature-
162 programmed oxidation (TPO) in a TA Instruments TGA-Q 5000 thermobalance.

163 *2.4. Reaction indexes*

164 Conversion (X) has been defined as the percent of LCO and HCO fractions in the feed
165 cracked to lighter products and condensed to coke:

$$X(wt\%) = \frac{(LCO + HCO)_{feed} - (LCO + HCO)_{prod}}{(LCO + HCO)_{feed}} 100 \quad (1)$$

The yield of each fraction ($Y_{fraction}$) has been defined as the mass ratio of each particular fraction referred to the total mass fed:

$$Y_{fraction}(wt\%) = \frac{mass_{fraction}}{mass_{total}} 100 \quad (2)$$

The values for the yields of each fraction obtained experimentally ($Y_{fraction}$) have been compared with those theoretically expected, i.e., $(Y_{fraction})_{theoretical}$. The latter, have been computed from the experimental yields obtained in the cracking of each component individually considering their content in the blend:

$$(Y_{fraction})_{theoretical} = 0.8 (Y_{fraction})_{VGO} + 0.2 (Y_{fraction})_{waxes} \quad (3)$$

where $(Y_{fraction})_{VGO}$ and $(Y_{fraction})_{waxes}$ are the yields of each fraction obtained in the cracking of pure VGO and HDPE waxes, respectively. These results have been reported in a previous work [37].

The calculation of the theoretical concentrations of the different fractions of products has been also performed according to weighted arithmetic mean. Finally, the research octane number (RON) of the naphtha fraction has been determined according to the procedure established by Anderson et al. [43].

3. Results and discussion

3.1. Conversion and yield of the products

In order to investigate the effect of the operating conditions (reaction temperature and C/O ratio) on the catalytic cracking reactions, the HDPE waxes/VGO blend has been

subjected to various experimental runs. Obtained results have been collected in Table 1 and compared with those obtained in the cracking of VGO, i.e., the current industrial FCC unit feedstock. Note that the values shown in Table 1 have been obtained after repeating each of the experiments at least three times and that show a SD of 2 %. Attending to obtained results, it can be seen that attained conversion are within the 40.6-66.3 wt% range for the blend and 41.4-62.7 wt% for the VGO. The effect of the operating conditions is of great relevance, as at low and mild-severity cracking conditions (500 and 530 ºC; and C/O = 3 and 5 g_{cat} g_{feed}^{-1}) the conversion attained in the cracking of the VGO is higher than that of the blend. However, this tendency is reversed at high-severity cracking conditions (specifically at 560 ºC). Hence, bigger differences have been obtained at 560 ºC and 3 g_{cat} g_{feed}^{-1} where the conversion obtained with the VGO is 2.2 wt% higher than that of the blend and at 560 ºC and 7 g_{cat} g_{feed}^{-1} where the conversion of the blend is 3.6 wt% higher than the conversion of the VGO.

Table 1. Conversion obtained at different temperatures and C/O ratios in the catalytic cracking of the HDPE waxes/VGO blend and of VGO.

	HDPE waxes/VGO			VGO[a]		
C/O ratio (g_{cat} g_{feed}^{-1})	500 ºC	530 ºC	560 ºC	500 ºC	530 ºC	560 ºC
3	40.6	49.3	57.6	41.4	51.1	59.8
5	43.9	51.6	63.1	44.2	53.4	61.1
7	47.6	55.5	66.3	47.3	55.5	62.7

[a] Data obtained from ref. [37].

The differences obtained in the cracking of both feeds rely on the different mechanisms they follow. This way, in the cracking of the VGO the formation of carbenium ions from olefins proceeds by addition of the proton from a Brønsted-type acid site to the carbon–carbon double bond of the olefin [44]. Afterwards, adsorbed carbenium ion will follow

206 either β-scission mechanism or protonated cyclopropane mechanism forming smaller
207 molecules [45]. Additionally, adsorbed carbenium species can easily oligomerize forming
208 bigger molecules that will be cracked afterwards, enhancing the activity of the catalyst
209 [46].

210 On the other hand, thermal cracking of HDPE waxes occurs through free radicals
211 mechanisms [47], whereas catalytic cracking proceeds through a carbocationic
212 mechanism [48]. This may occur directly at Lewis-type acid sites or by means of
213 previously adsorbed carbenium ions reacting with paraffins in a bimolecular-type of
214 mechanism [46]. However, the latter mechanism can only take place if the pore size of
215 the catalyst is large enough to accommodate the necessary reaction intermediates [45].
216 Therefore, high temperatures will boost the thermal cracking route of the HDPE waxes;
217 together with the catalytic one as shape restrictions are avoided. Moreover, the indirect
218 formation of carbenium ions [49] will also contribute to the higher conversion reached by
219 the blend when increasing the cracking severity.

220 Furthermore, as bulky molecules are found in the VGO, the possibility of the process
221 being influenced by mass transport phenomena in the microporous network cannot be
222 dismissed [50].

223 Figure 1 depicts the evolution of the yields of the main product fractions (dry gas, LPG,
224 naphtha, LCO, HCO and coke) with conversion in both the cracking of the blend and of
225 the VGO, which consists in a common approach to show the results obtained in the
226 catalytic cracking of hydrocarbon-based feeds [36]. Indeed, the use of conversion as a
227 variable allows for monitoring the evolution of the yields of products with the reaction
228 extent.

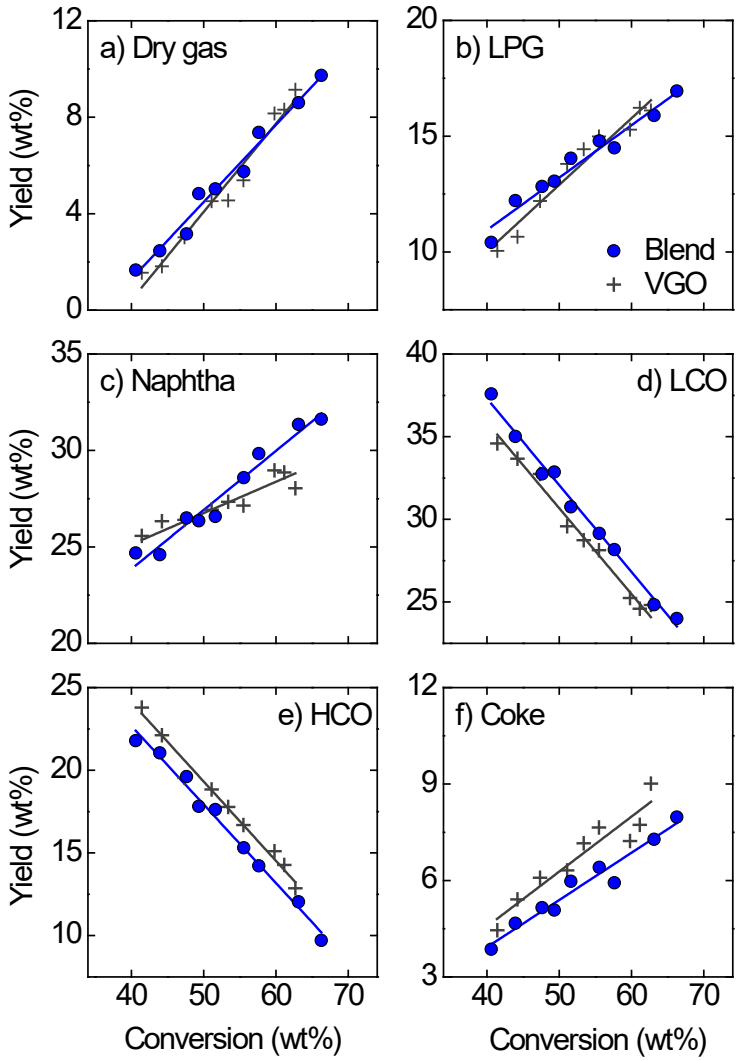

Figure 1. Comparison of the evolution with the conversion of the yields of dry gas (a), LPG (b), naphtha (c), LCO (d), HCO (e), and coke (f), in the catalytic cracking of the HDPE waxes/VGO blend (stuffed points) and of VGO (crosses). The standard deviation of the results in triplicate experimental replicates is below ± 2% of the average value.

The yields of both dry gas and LPG fractions (Figure 1a and b, respectively) follow the same trend with conversion, being higher their yield for the blend at conversion levels below 50 wt% but lower at higher conversion levels (X > 50 wt%). These results expose that in the cracking of the blend the over-cracking of the naphtha fraction is faster at low temperatures and low values of C/O ratio given the composition of the feedstock, i.e., more aliphatic and less aromatic than the VGO. On the contrary, the evolution of the

naphtha yield with the extent of reaction (Figure 1c) follows the opposite tendency. This way, for conversion values below 50 wt%, the naphtha yield obtained for the blend is lower than that obtained for the VGO. However, when increasing the cracking severity, the yield of naphtha obtained with the blend is higher. Hence, a notorious difference in the kinetics followed by the components of the blend can be assumed, which suggests certain synergism in the cracking mechanism. Similar tendencies were observed by Passamonti and Sedran [51] in the catalytic cracking of low-density polyethylene (LDPE) blended with VGO.

With regard to the yields of the LCO and HCO fractions (Figure 1d and e, respectively), the yield of LCO is ca. 1 wt% higher for the blend, whereas the yield of HCO is averagely 1 wt% lower. These differences are in concordance with the different composition of both feeds, as the content of LCO is 1.9 wt% higher and that of HCO 2.7 wt% lower for the HDPE waxes/VGO blend.

For the whole range of investigated operating conditions, i.e., all the conversion levels, the yield of coke fraction (Figure 1f) is averagely 1 wt% lower for the blend than for the VGO. The lower yield of coke can be attributed to the lower content of poly-aromatics within the HCO fraction, which are commonly known for being coke precursors [52]. The lower content of coke in the cracking of the blend is also a consequence of the different coke formation mechanisms followed by the hydrogenated chains of the HDPE waxes, as they will attenuate the rate of the aromatics condensation reactions. This asseveration has been ratified by Rodríguez et al. [53] when analyzing the nature of the coke formed in the cracking of VGO, HDPE waxes and the blend thereof. They have observed that the coke formed in the cracking of the HDPE waxes/VGO blend is less aromatic, more aliphatic, and with the presence of long olefinic chains.

In order to assess the existence of synergistic effects between both feeds, obtained experimental values have been compared with those theoretically expected according to the initial distributions of the fractions (Figure S1). Bigger differences between experimental and theoretical results are observed for the naphtha, LCO, HCO and coke fractions (Figure S1 c, d, e and f, respectively). The low content of coke (Figure S1f) will have an impact not only on the regeneration stage and, consequently, on the energy balance of the unit, but on the deactivation of the catalyst. The synergetic effects that affect the deposition of coke rely on the higher H/C ratio of the HDPE waxes dissolved in the VGO, which attenuate the coke formation mechanisms [54]. On the contrary, experimental yield of HCO fraction (Figure S1e) is higher than the expected one, specifically under low and medium-severity operating conditions. This result is a consequence of the (i) lower conversion of the molecules of this fraction into coke; and (ii) inhibition of the cracking reactions of the components within the HCO fraction because of the competitive adsorption on the acid sites of the waxes and of the heavy molecules of the VGO. This latter phenomenon has been also observed by Corma et al. [55] in the cracking of blends of naphtha and VGO.

With regard to LCO fraction (Figure S1d), a lower yield (~ 1 wt%) than that expected has been obtained for the whole range of investigated operating conditions. The inhibition of the cracking reactions of the components within the HCO fraction strongly influences the formation of LCO fraction. Besides, the co-feeding of HDPE waxes boosts the cracking of the LCO components towards lighter molecules promoting the formation of the naphtha fraction. This way, the yield of the naphtha fraction (Figure S1c) follows the same trend than that of the coke fraction, i.e., increases with the cracking severity. Indeed, experimental values are higher than those theoretically expected for conversion values higher than 50 wt%. Once again, deactivation of the catalyst and its over-cracking activity

play a key role in the formation of the naphtha fraction.

3.2. Yields of the gas products

The effect of the operating conditions on the cracking of the HDPE waxes/VGO blend on the yields of the gas products has been analyzed in Figure 2. Note that *n*-butene has been grouped together with *iso*-butene (clearly majority) given the slight difference between their boiling points (0.4 ºC) and the difficulty for their rigorous separation with the analysis system. However, the yields of *cis*-butene (*c*$C_4^=$) and *trans*-butene (*t*$C_4^=$) do have been quantified separately. Main gases have been ethylene ($C_2^=$) propylene ($C_3^=$) and *iso*-butane (*i*C_4), being their yields within the 0.8-4.5 wt%, 3.1-6.7 wt% and 0.7-4-4 wt% ranges, respectively. Attending to the effect of the operating conditions, an increase of the temperature boosts cracking reactions, inhibiting, at the same time, the hydrogen-transfer ones, which leads to the formation of olefins and C_1-C_2 paraffins in detriment of the C_3-C_4 paraffins. It should be highlighted that at 500 and 530 ºC *i*C_4 is the main product of the LPG fraction, whereas at 560 ºC the product with the higher yield is *i*$C_4^=$. This result lies on the boosting of cracking reactions at higher temperatures that lead to the formation of olefins from saturated compounds and to the attenuation of the hydrogen-transfer reactions that would convert the olefins into the corresponding paraffin [56]. C/O ratio has a lower effect on obtained conversions, at higher values of C/O the formation of the C_1-C_3 compounds together with C_4 paraffins and *iso*-butane is boosted, reducing the yields of the remaining butenes.

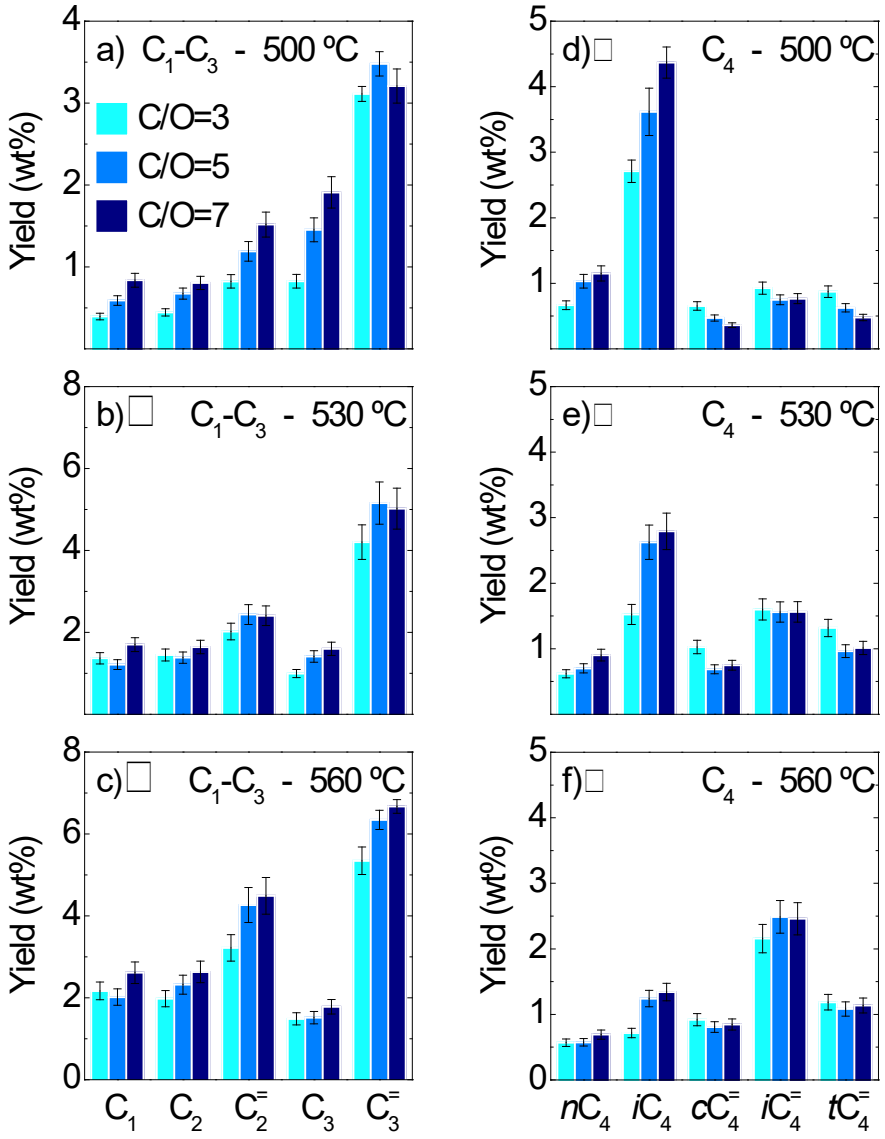

Figure 2. Evolution of the yields of C_1-C_4 products with C/O ratio in the catalytic cracking of the HDPE waxes/VGO blend. Graphs (a) and (d) correspond to 500 ºC, (b) and (e) to 530 ºC, and (c) and (f) to 560 ºC. The error bars represent the standard deviation of triplicate experimental replicates.

Comparing the results obtained for the blend (Figure 2) with those previously reported in the literature for the cracking of VGO [37], the yields of C_1-C_3 paraffins are similar for both feeds, being slightly higher the yield of methane and slightly lower the one of ethane in the cracking of the VGO. The yields of ethylene, propylene and *n*&*iso*-butene are higher in the cracking of the blend, specifically at high-severity cracking conditions. The

olefinic nature of the gas products obtained with the blend is a consequence of the content of paraffins and olefins within the naphtha fraction and of the ability of the equilibrium catalyst to produce light olefins under the FCC conditions. Once again, obtained results expose that the co-feeding of HDPE waxes modifies the cracking mechanisms. In this regard, the cracking mechanism ratio (CMR), defined as the dry gas (C_1-C_2) to *iso*-butane ratio, has been determined for both feeds. This parameter is a measure of protolytic cracking to β-scission reactions as dry gas products reflect protolytic cracking, whereas *iso*-butane reflects the formation of products through β-scission of branched hydrocarbons [57]. Higher values of CMR have been obtained for the blend, specifically at high temperatures and low C/O ratios, indicating that the co-feeding of HDPE waxes promotes the protolytic cracking route instead of the β-scission pathway.

Among the gas products, olefins are of great importance given the interest for their industrial utilization to produce a huge amount of relevant products on the daily lives of all global citizens [58]. In this context, the olefinicity of the LPG fraction has been determined ($C_3^=/C_{3-Total}$ and $C_4^=/C_{4-Total}$ mass ratios, respectively) and collected in Table 2. Temperature has a marked effect on the parameter for the C_4 isomers, whereas is less significant for the C_3 isomers. With regard to the effect of the C/O ratio, higher values decrease the olefinicity of the gas products, with a higher effect on C_4 products than on C_3 ones. This result exposes that hydrogen-transfer reactions are more active for butenes than for propene. Furthermore, similar values for the olefinicity have been obtained in the literature in the catalytic cracking of VGO [59] or vacuum residue (VR) [60].

Table 2. Effect of the reaction conditions on the olefinicity of the LPG fraction obtained in the catalytic cracking of the HDPE waxes/VGO blend.

$C_3^=/C_{3-Total}$			
T (°C)	C/O = 3 $g_{cat}\ g_{feed}^{-1}$	C/O = 5 $g_{cat}\ g_{feed}^{-1}$	C/O = 7 $g_{cat}\ g_{feed}^{-1}$
500	0.79	0.71	0.63
530	0.81	0.79	0.76
560	0.78	0.81	0.79
$C_4^=/C_{4-Total}$			
T (°C)	C/O = 3 $g_{cat}\ g_{feed}^{-1}$	C/O = 5 $g_{cat}\ g_{feed}^{-1}$	C/O = 7 $g_{cat}\ g_{feed}^{-1}$
500	0.48	0.36	0.28
530	0.73	0.56	0.55
560	0.83	0.77	0.76

3.3. Composition of the naphtha fraction

The chemical nature of the naphtha fraction has been determined by means of gas chromatographic analysis and obtained results have been collected in Figure 3. Main families of compounds are *iso*-paraffins, olefins and aromatics, but their concentration strongly depend on the temperature. This way, at 500 ºC the naphtha shows an *iso*-paraffinic (*i*-P) nature, aromatic (A) at 530 ºC and olefinic (O) at 560 ºC. However, *n*-paraffins (*n*-P) and naphthenes (N) are minority for the whole range of investigated operating conditions. Moreover, higher temperatures promote cracking reactions through β-scission and Diels-Alder cyclization reactions increasing the concentration of olefins and naphthenes, but inhibit the hydrogen-transfer ones and, hence, the formation of paraffins and aromatics from olefins and naphthenes [61]. On the other hand, an increase in the C/O ratio promotes the formation of *iso*-paraffins and aromatics, specifically at 500 and 530 ºC as hydrogen-transfer and dehydrogenation reactions are boosted. Obtained tendencies are in concordance with those previously obtained by Arandes et al. [62] in the catalytic cracking of polypropylene (PP) waxes under conditions similar to the ones

tested in this work.

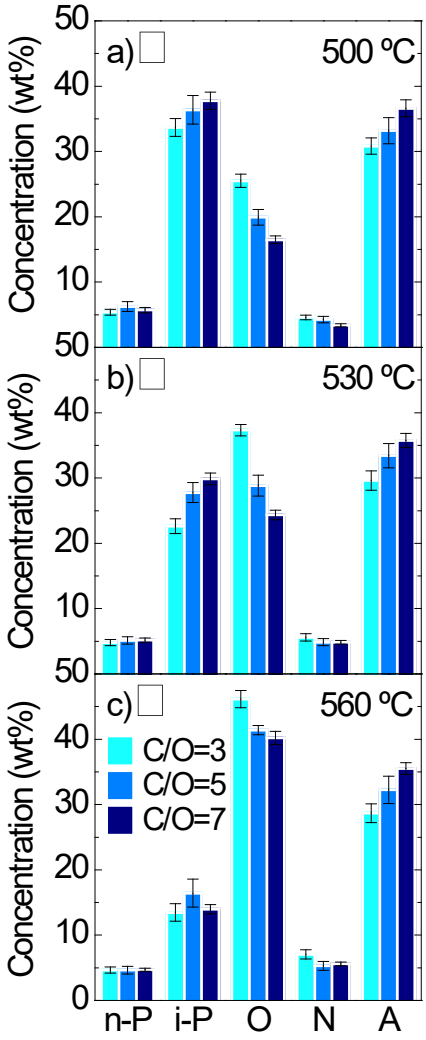

Figure 3. Effect of the C/O ratio on the composition of the naphtha fraction obtained in the cracking of the HDPE waxes/VGO blend at (a) 500 ºC, (b) 530 ºC, and (c) 560 ºC. Key: *n*-P, *n*-paraffins; *i*-P, *iso*-paraffins; O, olefins; N, naphthenes; and, A, aromatics. The error bars represent the standard deviation of triplicate experimental replicates.

The distribution of the families obtained in the catalytic cracking of the blend (Figure 3) is rather different than that previously reported when feeding VGO [37]. Likewise, the naphtha obtained when the HDPE waxes are co-fed is less aromatic for the whole range of operating conditions. However, the average difference is reduced at higher temperature, being of 8.7 wt% at 500 ºC and it is reduced to 7.6 and 4.8 wt% at 530 and 560 ºC,

371 respectively. Consequently, the concentration of *iso*-paraffins and olefins are higher in the
372 products obtained with the blend, but their distribution is strongly temperature-dependent.
373 This way, at 500 ºC *iso*-paraffins are clearly higher for the blend than for the VGO,
374 whereas at 560 ºC olefins prevail in the blend. On the other hand, the effect of the C/O
375 ratio is not that obvious and reduces the differences among the concentration of *n*-
376 paraffins, olefins and naphthenes.

377 Once again, the existence of synergistic effects has been ratified by comparing the
378 experimental results with the theoretically estimated ones (Figure S2). In this regard, the
379 co-feeding of HDPE waxes modifies the tendency followed by the different hydrocarbon
380 families when increasing the temperature because of the boost/inhibition of the hydrogen-
381 transfer and cracking reactions. This way, at 500 ºC the addition of the HDPE waxes
382 promotes the hydrogen-transfer reactions, obtaining higher concentrations of naphthenes
383 and olefins than those expected, and lower of *iso*-paraffins. Nevertheless, at 560 ºC
384 cracking reactions of heavier fractions, i.e., LCO and HCO, are promoted, specifically
385 the cracking of HDPE waxes-derived heavy molecules as it can be deduced from the
386 higher concentrations of olefins and naphthenes and lower of *iso*-paraffins. This
387 interpretation justifies that at 530 ºC an intermediate situation is reached, in which both
388 hydrogen-transfer and cracking reactions are relevant. Therefore, the content of *iso*-
389 paraffins is relevant at this temperature. Finally, the concentration of aromatics is lower
390 than the estimated one for the whole range of operating conditions because the
391 preferential cracking of the chains of HDPE waxes inhibits the dealkylation reactions that
392 form aromatics.

393 For more detailed information of the operating conditions on the composition of the
394 naphtha fraction, the different chemical families have been analyzed grouping them
395 according to the number of the carbon atoms (Figure 4 and 5). The distribution of *n*-

paraffins (Figure 4a-c) corresponds to a decreasing order from lower to higher number of carbon atoms. An increase of the temperature inhibits the formation of linear paraffins through hydrogen-transfer reactions, hence, the concentration of C_5-C_{10} *n*-paraffins decreases. However, the concentration of C_{11-12} *n*-paraffins increases because they are directly obtained through cracking of bigger paraffins within the LCO and HCO fractions. On the other hand, higher C/O ratios increase the formation of C_5-C_6 *n*-paraffins at 500 and 530 ºC, as hydrogen-transfer reactions are selectively promoted. For the remaining *n*-paraffins, there is not a clear predominance between cracking and hydrogen-transfer reactions. However, C_{11-12} *n*-paraffins are the exception, as cracking reactions are once again the predominant ones among them.

Iso-paraffins (Figure 4d-f) show a decreasing distribution from lower to higher number of carbon atoms, such as that previously discussed for *n*-paraffins. Moreover, both temperature and C/O ratio have similar effects on their concentration than those on *n*-paraffins, because of the key role of the hydrogen-transfer reactions. Consequently, the concentration of C_5-C_8 *iso*-paraffins decreases at higher temperatures, whereas the concentration of C_5 and C_7 *iso*-paraffins increases at higher C/O ratios. The increase of the C_9 *iso*-paraffins coincides with the decrease of the C_9 *n*-paraffin, which can be attributed to a boosting of the isomerization reactions.

As a consequence of the effect of the hydrogen-transfer reactions on the transformation of *n*-paraffins into olefins, the evolution of the concentration of olefins in the naphtha fraction with the temperature and C/O ratio (Figure 5a-c) is just the opposite to those of *n*- and *iso*-paraffins (Figure 4). This way, the concentration of olefins, which also follows a decreasing order from lower to higher number of carbon atoms, increases with temperature. On the contrary, the concentration of olefins decreases when increasing the C/O ratio, with the exception of the C_{10} olefins, whose formation is boosted as previously

explained for the $C_{10\text{-}12}$ *n*-paraffins.

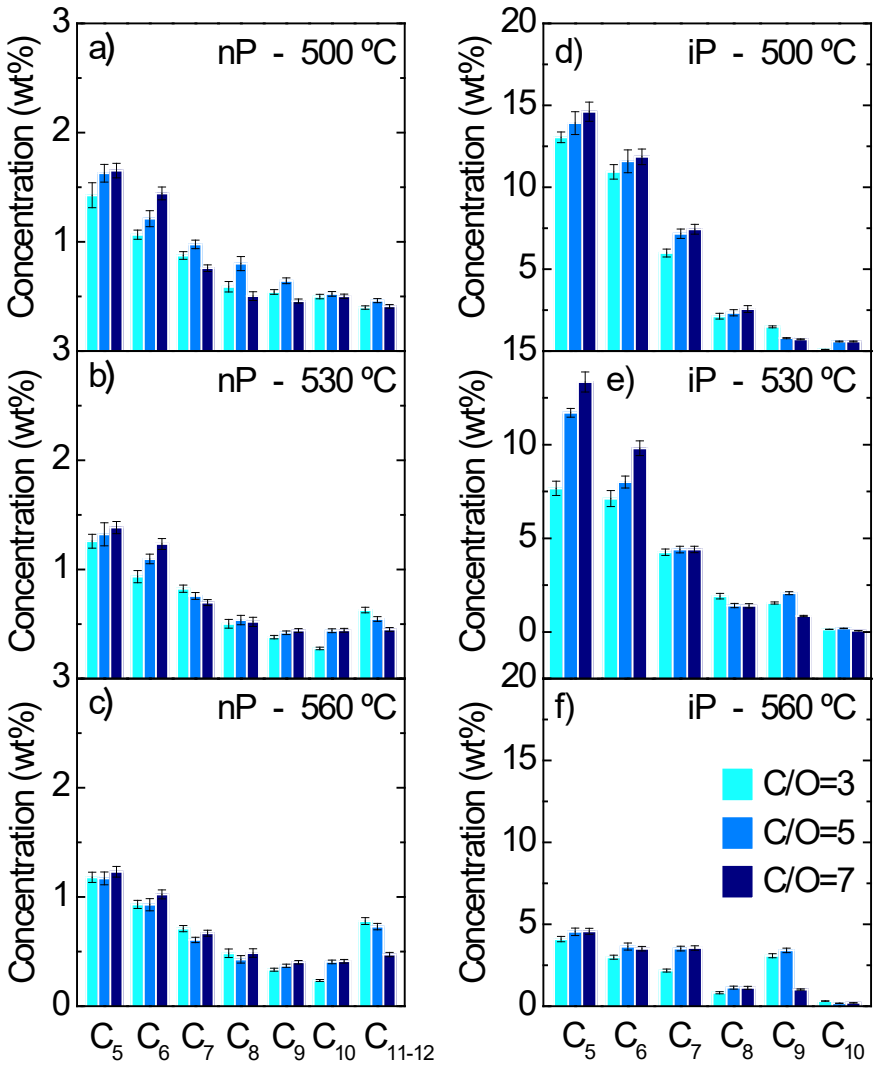

Figure 4. Evolution with C/O ratio of the concentration of *n*-paraffins (graphs a–c) and of *iso*-paraffins (graphs d–f) in the naphtha fraction grouped according to the number of carbon atoms at (graphs a and d) 500 ºC, (b and e) 530 ºC, and (graphs c and f) 560 ºC. Key: *n*-P, *n*-paraffins; *i*-P, *iso*-paraffins. The error bars represent the standard deviation of triplicate experimental replicates.

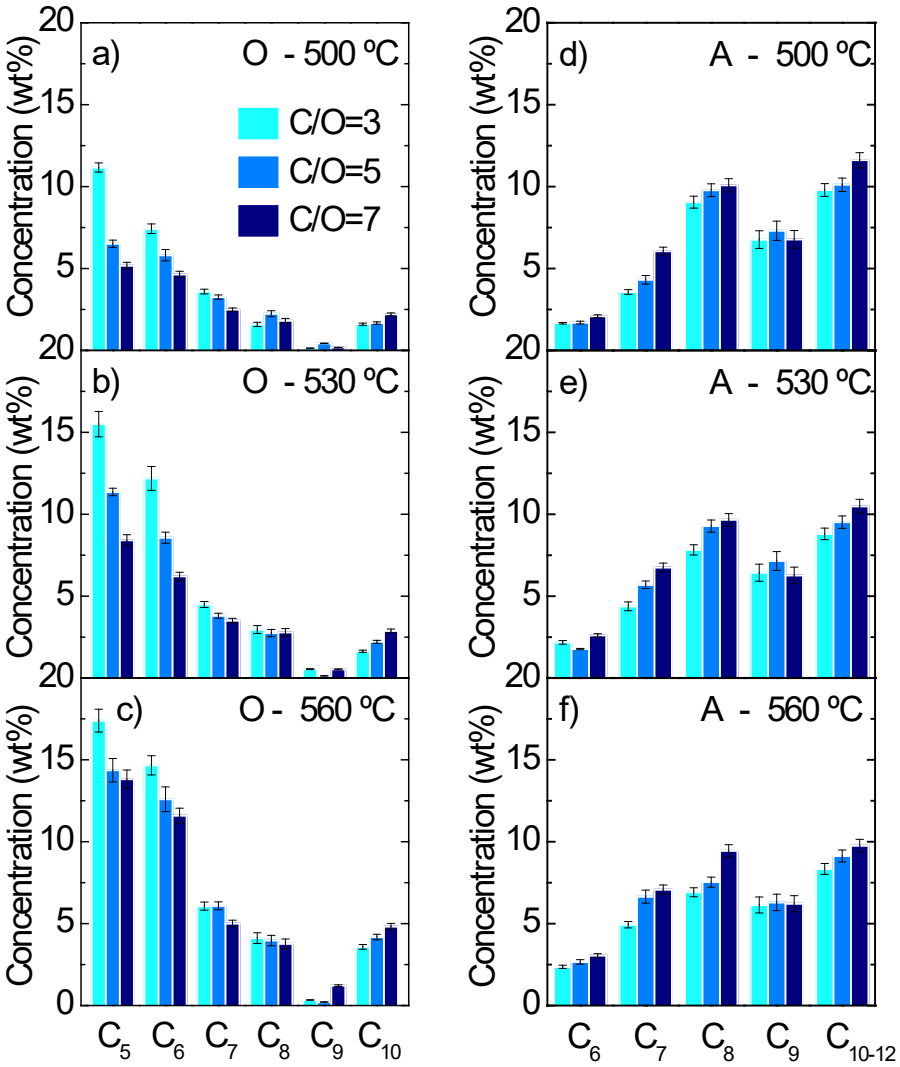

Figure 5. Evolution with C/O ratio of the concentration of olefins (graphs a–c) and of aromatics (graphs d–f) in the naphtha fraction grouped according to the number of carbon atoms at (graphs a and d) 500 ºC, (b and e) 530 ºC, and (graphs c and f) 560 ºC. Key: O, olefins; A, aromatics. The error bars represent the standard deviation of triplicate experimental replicates.

Within the aromatics, those with higher concentrations are the C_8 and C_{10-12} ones (Figure 5d-f). An increase in temperature promotes the dealkylation reactions of the heavy aromatics lateral chains, leading to a homogenization in the distribution of the number of carbon atoms. Hence, the formation of C_6 and C_7 aromatics, i.e., benzene and toluene, is

promoted. On the other hand, higher C/O ratios bring higher concentrations of aromatics, because dehydrogenation reactions that convert naphthenes into aromatics are favored. However, C_9 aromatics do not follow this trend as their concentration goes through a maximum at C/O = 5 g_{cat} g_{feed}^{-1}.

The aforementioned synergistic effects of the co-feeding of HDPE waxes also have a strong influence on the distribution of the number of carbon atoms for the different families. This way, the total amount of *n*-paraffins (Figure S2) is not that affected by the co-feeding of HDPE waxes, but it does the distribution of the number of carbon atoms (Figure S3). Despite the fact that the co-feeding promotes the hydrogen-transfer reactions at low temperatures, in the 500-530 ºC range experimental concentrations are lower than those theoretically estimated, with the exception of the C_{10} *n*-paraffin and other specific cases. From this result, it can be deduced that the cracking of the components of the VGO are inhibited at low temperatures. However, at 560 ºC both differences between experimental and weighted values are reduced, showing that both the components of the HDPE waxes and of the VGO are cracked.

Attending to *iso*-paraffins (Figure S4), obtained differences rely on the same mechanisms as those of the *n*-paraffins. This way, different tendencies are observed at 500-530 ºC and 560 ºC. At low temperature, when the distribution of *n*-paraffins and olefins is controlled by the hydrogen-transfer reactions, experimental results are higher than theoretical ones, showing that the co-feeding of HDPE waxes promotes this type of reactions. On the contrary, at 560 ºC hydrogen-transfer reactions are thermodynamically limited and cracking rates of the components of the VGO in the blend are sufficiently high to promote the formation of linear paraffins instead of ramified ones. Therefore, experimental values are below computed ones. In any case, these global criteria have some exceptions among the whole group of *iso*-paraffins analyzed, which can be attributable to synergetic effects

463 of the co-feeding affecting to other minority reactions, such as isomerization reactions.

464 Hydrogen-transfer reactions also play a key role in the distribution of the concentration
465 of olefins as depicted in Figure S5. Likewise, at 500 ºC the formation of both *n*- and *iso*-
466 paraffins is promoted, hence the experimental concentrations of olefins are below the
467 expected values. At 530 ºC this latter situation is only observed for C/O = 7 g_{cat} g_{feed}^{-1},
468 when hydrogen-transfer reactions are still the main ones. Contrarily, for smaller values of
469 C/O and, specifically, at 560 ºC (for the whole range of C/O ratios studied) experimental
470 values are higher than theoretical ones because of the aforementioned thermodynamic
471 restrictions of the hydrogen-transfer reactions.

472 Finally, the concentration of aromatics (Figure S6) does not follow any marked tendency
473 and attending to the evolution of the different groups can be obtained a complementary
474 explanation to that given before of the mechanisms that describe their evolution.
475 Therefore, the concentration of the C_8-C_9 aromatics is rather smaller than theoretical one,
476 which affects to the total amount of aromatics obtained, as well as their distribution
477 according to the number of carbon atoms. Consequently, the concentration of C_6, C_7 and
478 C_{10-12} aromatics is higher depending on the operating conditions tested. Then it can be
479 stated that the co-feeding of HDPE waxes promotes the preferential adsorption of the
480 waxes on the catalyst surface, resulting in the inhibition of the C_{10-12} aromatics lateral
481 chains at low temperature and in the boosting of the dealkylation of C_8-C_9 aromatics to
482 produce C_6 and C_7 aromatics at high temperature [63].

483 *3.4. Quality indexes of the naphtha fraction*

484 Several indexes have been computed to determine the quality of the naphtha fraction
485 obtained in the cracking of the HDPE waxes/VGO blend (Table 3). First of them is the
486 *iso*-paraffinicity index, which is defined as the *iso*-paraffins to *n*-paraffins index for the

487 molecules with 5, 6, 7 and 8 carbon atoms. Globally, highest *iso*-paraffinicity values have
488 been obtained at low temperature (500 ºC) and they decrease with temperature. However,
489 there is not a marked tendency when increasing the C/O ratio, as several times the highest
490 value has been obtained at the intermediate C/O ratio (5 g_{cat} g_{feed}^{-1}). Furthermore, obtained
491 values are similar to those obtained for the VGO but a bit lesser than them, but at 500 ºC
492 the values obtained with the blend are higher [37].

493 With regard to olefinicity, it tended to increase with reactor temperature while processing
494 at the lowest C/O ratio (3 g_{cat} g_{feed}^{-1}). This is, indeed, as expected development since
495 temperature promotes the β-scission reactions leading to enhanced olefins formation from
496 the cracking of long chains of paraffins and olefins [64]. Assessing the effect of the co-
497 feeding of the HDPE waxes, it can be seen that at 500 and 530 ºC it has little or no impact,
498 but at 560 ºC the impact of the addition of the polymer appears more visible. On the other
499 hand, the branching degree of the olefins has no marked tendency with temperature,
500 neither with C/O ratio. This absence of tendency is a consequence of the attenuation of
501 the hydrogen-transfer reactions when the polymer is co-fed, leading to a secondary place
502 the selective cracking of ramified olefins.

503 Finally, the most relevant index is the research octane number (RON) as it describes the
504 behavior of the fuel in the engine and is an attempt to simulate acceleration behavior. This
505 index increases both with temperature and C/O ratio, reaching considerably high values
506 within the 104.4-105.3 range at 560 ºC. These values are similar to those reported in the
507 catalytic cracking of the VGO [37].

508

509

510 **Table 3.** Effect of the reaction conditions on the quality indexes that characterize the
511 naphtha fraction obtained in the catalytic cracking of the HDPE waxes/VGO blend.

	T (ºC)	C/O=3	C/O=5	C/O=7
iso-paraffinicity				
	500	9.14	8.85	8.85
iC_5/nC_5	530	6.09	8.55	8.08
	560	3.47	3.88	3.72
	500	10.27	9.56	8.22
iC_6/nC_6	530	7.61	7.30	6.80
	560	3.20	3.91	3.43
	500	6.84	7.34	9.80
iC_7/nC_7	530	5.16	5.80	5.80
	560	3.06	5.40	5.31
	500	3.62	2.91	5.10
iC_8/nC_8	530	3.80	2.72	2.78
	560	1.70	2.65	2.30
olefinicity				
	500	0.44	0.30	0.24
$C_5^{=}/C_{5\ Total}$	530	0.63	0.47	0.36
	560	0.77	0.72	0.70
	500	0.35	0.29	0.23
$C_6^{=}/C_{6\ Total}$	530	0.54	0.44	0.31
	560	0.70	0.64	0.60
iso-olefinicity				
	500	1.12	0.95	0.94
$iC_5^{=}/nC_5^{=}$	530	1.15	1.04	0.91
	560	1.00	0.88	1.05
	500	0.63	0.29	0.28
$iC_6^{=}/nC_6^{=}$	530	0.64	0.56	0.35
	560	0.39	0.23	0.27
	500	0.27	0.19	0.19
$iC_7^{=}/nC_7^{=}$	530	0.21	0.18	0.18
	560	0.27	0.25	0.28
RON				
	500	102	102	103
	530	103	104	104
	560	104	105	105

4. Conclusions

The co-cracking of 20 wt% of HDPE waxes with VGO under conditions of the industrial FCC unit has a remarkable effect on the conversion, distribution of products and composition of the LPG and naphtha fractions. Moreover, positive synergetic effects have been also determined, which could enhance the prospects of their posterior valorization in refineries. This way, the low reactivity of the chains of HDPE waxes inhibits the cracking rates of the components of the VGO obtaining lower conversion values at 500 and 530 ºC for the blend (40.6-47.6 and 49.3-55.5 wt%, respectively) than for the VGO (41.4-47.3 and 51.1-55.5 wt%, respectively). However, higher temperatures promote the cracking of waxes leading to a higher conversion for the blend than for the VGO (63.1-66.3 and 61.1-62.7 wt%, respectively). Furthermore, the co-feeding attenuates the over-cracking reactions within the LPG and naphtha fractions. Therefore, their yields are higher than those of the cracking of the VGO, whereas the yield of dry gases is lower. On the other hand, as waxes increase the H/C ratio and decrease the content of poly-aromatics in the feed, the yield of coke decreases.

Attending to the composition of the products and comparing them with those obtained in the cracking of VGO, the naphtha fraction has a higher content of paraffins and olefins and lower of aromatics. Consequently, the gas fraction obtained with the blend has a higher content of olefins, i.e., ethylene, propylene and butenes. Moreover, an increase of the temperature promotes the cracking of heavy molecules within the HDPE waxes leading to the formation of *n*-paraffins and olefins, and, in a lesser extent, of aromatics and *iso*-paraffins. Contrarily, an increase of the C/O ratio boosts the hydrogen-transfer

reactions, leading to an increase of the paraffins and aromatics concentration and a decrease of that of naphthenes and olefins.

Consequently, obtained results expose that proposed tandem strategy of pyrolysing waste plastic in a first stage to produce waxes, which will be afterwards cracked in a refinery FCC unit together with VGO is a promising strategy to treat the current environmental issues derived from the uncontrolled disposal and inefficient recycling strategies.

Acknowledgments

This work has been carried out with financial support of the Ministry of Science, Innovation and Universities (MICINN) of the Spanish Government (grant RTI2018-096981-B-I00), the Basque Government (grant IT1218-19) and the European Union's ERDF funds and Horizon 2020 research and innovation programme under the Marie Skłodowska-Curie Actions (grant No 823745).

David Trueba is grateful for his PhD grant awarded by the University of the Basque Country UPV/EHU (PIF 2018).

The authors also acknowledge Petronor Refinery for providing the VGO and the catalyst used in this work.

References

[1] PEMRG Plastics Europe's Market Research and Statistics Group. Plastics the facts 2019. An analysis of European plastics production, demand and waste data. Brussels: 2019.

554 [2] Barnes SJ. Understanding plastics pollution: The role of economic development
555 and technological research. Environ Pollut 2019;249:812–21.
556 doi:10.1016/j.envpol.2019.03.108.

557 [3] Gallo F, Fossi C, Weber R, Santillo D, Sousa J, Ingram I, et al. Marine litter plastics
558 and microplastics and their toxic chemicals components: the need for urgent
559 preventive measures. Environ Sci Eur 2018;30:13. doi:10.1186/s12302-018-0139-
560 z.

561 [4] Lopez G, Artetxe M, Amutio M, Bilbao J, Olazar M. Thermochemical routes for
562 the valorization of waste polyolefinic plastics to produce fuels and chemicals. A
563 review. Renew Sustain Energy Rev 2017;73:346–68.
564 doi:10.1016/j.rser.2017.01.142.

565 [5] Lopez G, Artetxe M, Amutio M, Alvarez J, Bilbao J, Olazar M. Recent advances
566 in the gasification of waste plastics. A critical overview. Renew Sustain Energy
567 Rev 2018;82:576–96. doi:10.1016/j.rser.2017.09.032.

568 [6] Grim RG, To AT, Farberow CA, Hensley JE, Ruddy DA, Schaidle JA. Growing
569 the bioeconomy through catalysis: A review of recent advancements in the
570 production of fuels and chemicals from syngas-derived oxygenates. ACS Catal
571 2019;9:4145–72. doi:10.1021/acscatal.8b03945.

572 [7] Zhou W, Cheng K, Kang J, Zhou C, Subramanian V, Zhang Q, et al. New horizon
573 in C1 chemistry: Breaking the selectivity limitation in transformation of syngas

574 and hydrogenation of CO_2 into hydrocarbon chemicals and fuels. Chem Soc Rev
575 2019;48:3193–228. doi:10.1039/C8CS00502H.

576 [8] Anuar Sharuddin SD, Abnisa F, Wand Daud WMA, Aroua MK. A review on
577 pyrolysis of plastic wastes. Energy Convers Manage 2016;115:308–26.
578 doi:10.1016/j.enconman.2016.02.037.

579 [9] Al-Salem SM, Antelava A, Constantinou A, Manos G, Dutta A. A review on
580 thermal and catalytic pyrolysis of plastic solid waste (PSW). J Environ Manage
581 2017;197:177–98. doi:10.1016/j.jenvman.2017.03.084.

582 [10] Fox JA, Stacey NT. Process targeting: An energy based comparison of waste plastic
583 processing technologies. Energy 2019;170:273–83.
584 doi:10.1016/j.energy.2018.12.160.

585 [11] Artetxe M, Lopez G, Elordi G, Amutio M, Bilbao J, Olazar M. Production of light
586 olefins from polyethylene in a two-step process: Pyrolysis in a conical spouted bed
587 and downstream high-temperature thermal cracking. Ind Eng Chem Res
588 2012;51:13915–23. doi:10.1021/ie300178e.

589 [12] Quesada L, Pérez A, Godoy V, Peula FJ, Calero M, Blázquez G. Optimization of
590 the pyrolysis process of a plastic waste to obtain a liquid fuel using different
591 mathematical models. Energy Convers Manage 2019;188:19–26.
592 doi:10.1016/j.enconman.2019.03.054.

593 [13] Fivga A, Dimitriou I. Pyrolysis of plastic waste for production of heavy fuel

substitute: A techno-economic assessment. Energy 2018;149:865–74. doi:10.1016/j.energy.2018.02.094.

[14] Chen W, Shi S, Zhang J, Chen M, Zhou X. Co-pyrolysis of waste newspaper with high-density polyethylene: Synergistic effect and oil characterization. Energy Convers Manage 2016;112:41–8. doi:10.1016/j.enconman.2016.01.005.

[15] Yang J, Rizkiana J, Widayatno WB, Karnjanakom S, Kaewpanha M, Hao X, et al. Fast co-pyrolysis of low density polyethylene and biomass residue for oil production. Energy Convers Manage 2016;120:422–9. doi:10.1016/j.enconman.2016.05.008.

[16] Damodharan D, Sathiyagnanam AP, Rana D, Kumar BR, Saravanan S. Combined influence of injection timing and EGR on combustion, performance and emissions of DI diesel engine fueled with neat waste plastic oil. Energy Convers Manage 2018;161:294–305. doi:10.1016/j.enconman.2018.01.045.

[17] Bharathy S, Gnanasikamani B, Radhakrishnan Lawrence K. Investigation on the use of plastic pyrolysis oil as alternate fuel in a direct injection diesel engine with titanium oxide nanoadditive. Environ Sci Pollut Res 2019;26:10319–32. doi:10.1007/s11356-019-04293-0.

[18] Kaimal VK, Vijayabalan P. A detailed study of combustion characteristics of a DI diesel engine using waste plastic oil and its blends. Energy Convers Manage 2015;105:951–6. doi:10.1016/j.enconman.2015.08.043.

614 [19] Gadwal SB, Banapurmath NR, Kamoji MA, Rampure PB, Khandal SV.
615 Performance and emission characteristic studies on CRDI diesel engine fuelled
616 with plastic pyrolysis oil blended with ethanol and diesel. Int J Sustain Eng
617 2019;12:262–71. doi:10.1080/19397038.2018.1527863.

618 [20] Kumar S, Prakash R, Murugan S, Singh RK. Performance and emission analysis
619 of blends of waste plastic oil obtained by catalytic pyrolysis of waste HDPE with
620 diesel in a CI engine. Energy Convers Manage 2013;74:323–31.
621 doi:10.1016/j.enconman.2013.05.028.

622 [21] Auxilio AR, Choo W-L, Kohli I, Chakravartula Srivatsa S, Bhattacharya S,
623 Srivatsa SC, et al. An experimental study on thermo-catalytic pyrolysis of plastic
624 waste using a continuous pyrolyser. Waste Manage 2017;67:143–54.
625 doi:10.1016/j.wasman.2017.05.011.

626 [22] Budsaereechai S, Hunt AJ, Ngernyen Y. Catalytic pyrolysis of plastic waste for the
627 production of liquid fuels for engines. RSC Adv 2019;9:5844–57.
628 doi:10.1039/C8RA10058F.

629 [23] Elordi G, Olazar M, Castaño P, Artetxe M, Bilbao J. Polyethylene cracking on a
630 spent FCC catalyst in a conical spouted bed. Ind Eng Chem Res 2012;51:14008–
631 17. doi:10.1021/ie3018274.

632 [24] Lee H, Park Y-K. Catalytic pyrolysis of polyethylene and polypropylene over
633 desilicated beta and Al-MSU-F. Catalysts 2018;8:501. doi:10.3390/catal8110501.

634 [25] Akubo K, Nahil MA, Williams PT. Aromatic fuel oils produced from the pyrolysis-
635 catalysis of polyethylene plastic with metal-impregnated zeolite catalysts. J Energy
636 Inst 2019;92:195–202. doi:10.1016/j.joei.2017.10.009.

637 [26] Artetxe M, Lopez G, Amutio M, Elordi G, Bilbao J, Olazar M. Light olefins from
638 HDPE cracking in a two-step thermal and catalytic process. Chem Eng J
639 2012;207–208:27–34. doi:10.1016/j.cej.2012.06.105.

640 [27] Wang J, Jiang J, Sun Y, Zhong Z, Wang X, Xia H, et al. Recycling benzene and
641 ethylbenzene from in-situ catalytic fast pyrolysis of plastic wastes. Energy Convers
642 Manage 2019;200. doi:10.1016/j.enconman.2019.112088.

643 [28] Yu D, Hui H, Li S. Two-step catalytic co-pyrolysis of walnut shell and LDPE for
644 aromatic-rich oil. Energy Convers Manage 2019;198.
645 doi:10.1016/j.enconman.2019.111816.

646 [29] Fan L, Zhang Y, Liu S, Zhou N, Chen P, Liu Y, et al. Ex-situ catalytic upgrading of
647 vapors from microwave-assisted pyrolysis of low-density polyethylene with MgO.
648 Energy Convers Manage 2017;149:432–41. doi:10.1016/j.enconman.2017.07.039.

649 [30] Ding K, Liu S, Huang Y, Liu S, Zhou N, Peng P, et al. Catalytic microwave-assisted
650 pyrolysis of plastic waste over NiO and HY for gasoline-range hydrocarbons
651 production. Energy Convers Manage 2019;196:1316–25.
652 doi:10.1016/j.enconman.2019.07.001.

653 [31] Aguado R, Prieto R, San José MJ, Alvarez S, Olazar M, Bilbao J. Defluidization

654 modelling of pyrolysis of plastics in a conical spouted bed reactor. Chem Eng
655 Process Process Intensif 2005;44:231–5. doi:10.1016/j.cep.2004.02.016.

656 [32] Aguado R, Olazar M, San José, MJ, Gaisán B, Bilbao J. Wax formation in the
657 pyrolysis of polyolefins in a conical spouted bed reactor. Energy Fuels
658 2002;16:1429–37. doi:10.1021/ef020043w.

659 [33] Elordi G, Olazar M, Lopez G, Artetxe M, Bilbao J. Product yields and
660 compositions in the continuous pyrolysis of high-density polyethylene in a conical
661 spouted bed reactor. Ind Eng Chem Res 2011;50:6650–9. doi:10.1021/ie200186m.

662 [34] Arabiourrutia M, Elordi G, Lopez G, Borsella E, Bilbao J, Olazar M.
663 Characterization of the waxes obtained by the pyrolysis of polyolefin plastics in a
664 conical spouted bed reactor. J Anal Appl Pyrolysis 2012;94:230–7.
665 doi:10.1016/j.jaap.2011.12.012.

666 [35] Passamonti FJ, de la Puente G, Sedran U. Reconversion of Olefinic Cuts from
667 Fluidized Catalytic Cracking Naphthas. Ind Eng Chem Res 2004;43:1405–10.
668 doi:10.1021/ie030467t.

669 [36] García JR, Falco M, Sedran U. Intracrystalline mesoporosity over Y zeolites.
670 Processing of VGO and resid-VGO mixtures in FCC. Catal Today 2017;296:247–
671 53. doi:10.1016/j.cattod.2017.04.010.

672 [37] Rodríguez E, Gutiérrez A, Palos R, Vela FJ, Arandes JM, Bilbao J. Fuel production
673 by cracking of polyolefins pyrolysis waxes under fluid catalytic cracking (FCC)

operating conditions. Waste Manage 2019;93:162–72. doi:10.1016/j.wasman.2019.05.005.

[38] Rodríguez E, Palos R, Gutiérrez A, Vela FJ, Arandes JM, Bilbao J. Effect of the FCC equilibrium catalyst properties and of the cracking temperature on the production of fuel from HDPE pyrolysis waxes. Energy Fuels 2019;33:5191–9. doi:10.1021/acs.energyfuels.9b00993.

[39] Rodríguez E, Gutiérrez A, Palos R, Azkoiti MJ, Arandes JM, Bilbao J. Cracking of scrap tires pyrolysis oil in a fluidized bed reactor under catalytic cracking unit conditions. Effects of operating conditions. Energy Fuels 2019;33:3133–43. doi:10.1021/acs.energyfuels.9b00292.

[40] De Lasa H. Riser Simulator, U.S. Patent. 5,102,628, 1992.

[41] Alkhlel A, De Lasa H. Catalytic cracking of hydrocarbons in a CREC riser simulator using a Y-zeolite-based catalyst: Assessing the catalyst/oil ratio effect. Ind Eng Chem Res 2018;57:13627–38. doi:10.1021/acs.iecr.8b02427.

[42] Rodríguez E, Palos R, Gutiérrez A, Arandes JM, Bilbao J. Production of non-conventional fuels by catalytic cracking of scrap tires pyrolysis oil. Ind Eng Chem Res 2019;58:5158–67. doi:10.1021/acs.iecr.9b00632.

[43] Anderson PC, Sharkey JM, Walsh RP. Calculation of the research octane number of motor gasolines from gas chromatographic data and a new approach to motor gasoline quality control. J Inst Pet 1972;58:83–94.

694 [44] Yokoi T, Mochizuki H, Namba S, Kondo JN, Tatsumi T. Control of the Al
695 distribution in the framework of ZSM-5 zeolite and its evaluation by solid-state
696 NMR technique and catalytic properties. J Phys Chem C 2015;119:15303–15.
697 doi:10.1021/acs.jpcc.5b03289.

698 [45] den Hollander MA, Wissink M, Makkee M, Moulijn JA. Gasoline conversion:
699 reactivity towards cracking with equilibrated FCC and ZSM-5 catalysts. Appl
700 Catal A Gen 2002;223:85–102. doi:10.1016/S0926-860X(01)00745-1.

701 [46] Williams BA, Babitz SM, Miller JT, Snurr RQ, Kung HH. The roles of acid
702 strength and pore diffusion in the enhanced cracking activity of steamed Y zeolites.
703 Appl Catal A Gen 1999;177:161–75. doi:10.1016/S0926-860X(98)00264-6.

704 [47] Shabtai J, Xiao X, Zmierczak W. Depolymerization−liquefaction of plastics and
705 rubbers. 1. Polyethylene, polypropylene, and polybutadiene. Energy Fuels
706 1997;11:76–87. doi:10.1021/ef960076+.

707 [48] Serrano DP, Aguado J, Escola JM. Developing advanced catalysts for the
708 conversion of polyolefinic waste plastics into fuels and chemicals. ACS Catal
709 2012;2:1924–41. doi:10.1021/cs3003403.

710 [49] Etim UJ, Bai P, Wang Y, Subhan F, Liu Y, Yan Z. Mechanistic insights into
711 structural and surface variations in Y-type zeolites upon interaction with binders.
712 Appl Catal A Gen 2019;571:137–49. doi:10.1016/j.apcata.2018.12.013.

713 [50] Zhang X, Cheng D, Chen F, Zhan X. The role of external acidity of hierarchical

714 ZSM-5 zeolites in n-heptane catalytic cracking. ChemCatChem 2018;10:2655–63.
715 doi:10.1002/cctc.201800086.

716 [51] Passamonti FJ, Sedran U. Recycling of waste plastics into fuels. LDPE conversion
717 in FCC. Appl Catal B Environ 2012;125:499–506.
718 doi:10.1016/j.apcatb.2012.06.020.

719 [52] Errekatxo A, Ibarra A, Gutierrez A, Bilbao J, Arandes JM, Castaño P. Catalytic
720 deactivation pathways during the cracking of glycerol and glycerol/VGO blends
721 under FCC unit conditions. Chem Eng J 2017;307:955–65.
722 doi:10.1016/j.cej.2016.08.100.

723 [53] Rodríguez E, Elordi G, Valecillos J, Izaddoust S, Bilbao J, Arandes JM, et al. Coke
724 deposition and product distribution in the co-cracking of waste polyolefin derived
725 streams and vacuum gas oil under FCC unit conditions. Fuel Process Technol
726 2019;192:130–9. doi:10.1016/j.fuproc.2019.04.012.

727 [54] Cerqueira HS, Caeiro G, Costa L, Ramôa Ribeiro F. Deactivation of FCC catalysts.
728 J Mol Catal A Chem 2008;292:1–13. doi:10.1016/j.molcata.2008.06.014.

729 [55] Corma A, Melo F V, Sauvanaud L, Ortega F. Different process schemes for
730 converting light straight run and fluid catalytic cracking naphthas in a FCC unit for
731 maximum propylene production. Appl Catal A Gen 2004;265:195–206.
732 doi:10.1016/j.apcata.2004.01.020.

733 [56] Passamonti FJ, de la Puente G, Sedran U. Factors influencing the isobutane yield

734 during the conversion of vacuum gas oil (VGO) under fluidized catalytic cracking
735 (FCC) conditions. Ind Eng Chem Res 2007;46:9269–73. doi:10.1021/ie070880r.

736 [57] Siddiqui MAB, Aitani AM, Saeed MR, Al-Yassir N, Al-Khattaf S. Enhancing
737 propylene production from catalytic cracking of Arabian light VGO over novel
738 zeolites as FCC catalyst additives. Fuel 2011;90:459–66.
739 doi:10.1016/j.fuel.2010.09.041.

740 [58] Sydora OL. Selective ethylene oligomerization. Organometallics 2019;38:997–
741 1010. doi:10.1021/acs.organomet.8b00799.

742 [59] Wallenstein D, Schäfer K, Harding RH. Impact of rare earth concentration and
743 matrix modification in FCC catalysts on their catalytic performance in a wide array
744 of operational parameters. Appl Catal A Gen 2015;502:27–41.
745 doi:10.1016/j.apcata.2015.05.010.

746 [60] Tang R, Yuan M, Liu K, Li H, Zhang J, Tian Y. Utilization of bifunctional catalyst
747 for upgrading petroleum residue via cracking and gasification: Effect of catalysts.
748 J Energy Inst 2018:In Press. doi:10.1016/j.joei.2018.11.001.

749 [61] Al-Sabawi M, De Lasa H. Modeling thermal and catalytic conversion of decalin
750 under industrial FCC operating conditions. Chem Eng Sci 2010;65:626–44.
751 doi:10.1016/j.ces.2009.08.035.

752 [62] Arandes JM, Torre I, Azkoiti MJ, Castaño P, Bilbao J, de Lasa H. Effect of catalyst
753 properties on the cracking of polypropylene pyrolysis waxes under FCC conditions.

754 Catal Today 2008;133–135:413–9. doi:10.1016/j.cattod.2007.12.080.

755 [63] Lovás P, Hudec P, Jambor B, Hájeková E, Horňáček M. Catalytic cracking of heavy
756 fractions from the pyrolysis of waste HDPE and PP. Fuel 2017;203:244–52.
757 doi:10.1016/j.fuel.2017.04.128.

758 [64] Odjo AO, García AN, Marcilla A. Refinery nonconventional feedstocks: Influence
759 of the coprocessing of vacuum gas oil and low density polyethylene in fluid
760 catalytic cracking unit on full range gasoline composition. Energy Fuels
761 2014;28:1579–93. doi:10.1021/ef4020394.

762